Journal of Sustainable Development of Energy, Water and Environment Systems

http://www.sdewes.org/jsdewes

Year 2022, Volume 10, Issue 2, 1090398

Original Research Article

Strontium Hexaferrite / Zinc Oxide Nanocomposites: Study on Photocatalytic Discoloration of Orange II Dye

Carlos A. Herme**, Silvia E. Jacobo

LaQuiMMAI (Laboratorio Químico de Materiales Magnéticos Aplicados a la Ingeniería), Facultad de Ingeniería de la Universidad de Buenos Aires

IQAI (Instituto de Química Aplicada a la Ingeniería), Universidad de Buenos Aires

Paseo Colón Ave. 850, C1063ACV Buenos Aires, Argentina

E-mail: cherme@fi.uba.ar, sjacobo@fi.uba.ar

Cite as: Herme, C. A., Jacobo, S. E. Strontium Hexaferrite / Zinc Oxide Nanocomposites: Study on Photocatalytic Discoloration of Orange II Dye, J. sustain. dev. energy water environ. syst., 10(2), 1090398, 2022, DOI: https://doi.org/10.13044/j.sdewes.d9.0398

ABSTRACT

Orange II is an azo dye widely used in the textile industry. Its discharge into water bodies is harmful to the ecosystem and causes a health hazard. The removal of organic pollutants from wastewater by photocatalyzed discoloration processes has been thoroughly studied. Notwithstanding, it would be interesting to support the catalyst on magnetic materials to facilitate its recovery. In the present work, catalytic discoloration of Orange II was performed using zinc oxide nanopowder in aqueous suspension and novel composites of zinc oxide supported on magnetic materials. We report a one-step method for the synthesis of composites by precipitation of zinc oxide on hard strontium ferrites, which may improve catalyst remotion from water without decreasing its catalytic performance. Composites were structurally and magnetically characterized. The discoloration process, scanned by spectrophotometry for six hours, followed first-order kinetics with a reaction rate constant of 0.0142 1/min and a half-life of 49 min for strontium ferrite/zinc oxide in neutral media at 25 °C. Orange II significant adsorption on catalysts was discarded. The composites showed great stability in aqueous suspension and excellent photocatalytic properties compared with zinc oxide. They can be easily removed from water by magnetic decantation, with a significant recovery factor (70%).

KEYWORDS

Photocatalytic discoloration, Zinc oxide, Azo dye, Visible light photocatalysis, Magnetic nanoparticles, Strontium hexaferrite, Composites.

INTRODUCTION

Orange II, also known as 2-Naphthol Orange and Acid Orange 7, is an important example of azo compound dye. It is widely used in wool dyeing and as a colouring agent in printing. Its discharge in water bodies after the industrial operations causes severe damage to aquatic environments and provokes health hazards.

Among the different azo dyes, Orange II was chosen for this study for many reasons. It could be easily prepared and purified in our laboratory. Its concentration in water can be easily measured by spectrophotometry because it has an absorbance maximum within the visible light

* Corresponding author

spectrum. In the darkness, it would not be oxidized or reduced by other components in the solution. In addition to this, this azo dye is not a pH indicator, so the hydronium concentration changes, which may happen in the discoloration process, will not shift its absorbance peak during the kinetics experiments.

Due to its high stability, Orange II is not easily biodegradable, and its discoloration requires special methods, as was reported by Daneshvar *et al.* [1]. The removal of organic pollutants from wastewater and effluents by discoloration processes using different photocatalysts was thoroughly studied by Khan *et al.* [2]. These processes would combine the adsorption of azo dye over the catalyst and its oxidative degradation in a photoreaction. Appropriate light irradiation over semiconductor oxides results in electron-hole pairs generation, which starts producing hydroxide radicals (•OH). Nishio *et al.* studied that these reactive agents can oxidize azo compounds to ammonium sulfate, carbon dioxide, and water without generating any solid waste [3].

Semiconductor metal oxides, such as titanium dioxide (TiO_2) and zinc oxide (ZnO), can act as good catalysts for azo dye oxidation due to their chemical stability, low toxicity, and high photosensitivity. Daneshvar *et al.* reported that ZnO has a higher photocatalytic efficiency compared with TiO_2 [4]. The effect of the preparation method on the catalytic activity of both semiconductor oxides was studied by Gonçalves *et al.* [5].

The use of zinc oxide nanoparticles as a catalyst of oxidation processes under sunlight exposition has been thoroughly studied, as it is reviewed by Ong *et al.* [6]. It is known that ZnO is an n-type semiconductor with a wideband gap of 3.37 eV and a large exciton binding energy of 60 meV [7].

ZnO, as a photocatalyst, has been tested in nanopowder aqueous suspension by Daneshvar *et al.* [1]. Marto *et al.* studied its activity supported on ceramic tiles [8]. Zinc oxide thin films were examined by Ali *et al.* [9]. Danwittayakul *et al.* used it in nanorods [10]. ZnO nanorods deposited onto borosilicate glass were studied by Sáenz-Trevizo *et al.* [11]. The activity of a zinc oxide microsphere suspension was measured by Wang *et al.* [12]. Whereas ceramic-supported ZnO microspheres were tested by Liu *et al.* [13].

The efficiency of zinc oxide as a catalyst depends on several factors. The effect of preparation methods was reported by Balcha *et al.* [14]. Sharma *et al.* examined the influence of annealing temperature [15]. The relation between ZnO activity and its particle size and morphology was studied by Kumar *et al.* [16].

Magnetic composites as catalyst support have been earlier prepared as it was informed in an article by Govan and Gun'ko [17]. Notwithstanding, along with all these supported catalysts, it seems necessary to protect the magnetic core to retain magnetic properties. For that reason, the core is coated with some non-magnetic relatively inert shell such as silica, as was reported by Faraji *et al.* [18]. The silica shell is straightforward to functionalize and suitable for binding various catalytic species, including transition metal complexes.

Catalyst remotion from water would be a desirable advantage, as Wu *et al.* reported [19]. Bacchetta *et al.* proved that ZnO nanoparticles could be harmful to different aquatic organisms [20]. Chevallet *et al.* studied the toxicity of zinc oxide on liver cells [21]. Whereas Kononenko *et al.* tested it on kidney cells [22].

The present work aims to explore the discoloration process of Orange II photocatalyzed by ZnO nanoparticles with two different strontium ferrite/zinc oxide composites prepared by a coprecipitation route. These magnetic phases were hexagonal ferrites (strontium ferrite and neodymium-cobalt strontium ferrite). We report a one-step method for synthesizing the composite Sr ferrite/ZnO as the magnetic phase is a hard ferrite with good chemical stability.

Spinel ferrites, soft ferromagnetic materials, have also been tested in wastewater treatment, as was reported by Kefeni *et al.* [23]. Among these materials, zinc ferrite ($ZnFe_2O_4$) was studied by Cai *et al.* as a photocatalyst of dyes degradation in the presence of persulfate [24]. The mechanism of this process has been studied by Zhu *et al.* [25]. Tadjarodi *et al.* tested the photocatalytic activity of zinc ferrite encapsulated in clay as a nanocomposite [26]. The use of

a ZnO/Zn ferrite composite as a catalyst has been published by Coelho *et al.* [27]. In comparison, Mandal and Natarajan studied the catalytic properties of a composite of ZnO and a Zn-Fe mixed oxide [28]. Zinc oxide composite catalysts with hematite (Fe_2O_3) or with elemental iron were tested by Maya-Treviño *et al.* [29]. All these composite catalysts were prepared with soft ferrites. Notwithstanding, the photocatalyzed discoloration of an azo dye by ZnO supported on hard ferrite particles, as it is informed in this work, would constitute a novel study. To the best of our knowledge, no similar system has been reported yet.

MATERIALS AND METHODS

Both phases of the composites were prepared using wet methods in our laboratory.

Preparation of strontium hexaferrite/zinc oxide composites

Strontium hexaferrite particles were synthesized by a self-combustion method, and the hydrated ZnO was precipitated on the magnetic support.

Synthesis of strontium hexaferrite and neodymium-cobalt substituted strontium hexaferrite. Samples of strontium hexaferrite (labelled as M00, with nominal composition $SrFe_{11}O_{19}$) and neodymium-cobalt substituted strontium hexaferrite (labelled M20, nominal composition $Sr_{0.8}Nd_{0.2}Co_{0.2}Fe_{10.8}O_{19}$) were synthesized using a self-combustion method reported by Herme *et al.* [30]. All the reactants, iron (III) nitrate nonahydrate ($Fe(NO_3)_3{\cdot}9H_2O$), strontium carbonate ($SrCO_3$), neodymium oxide (Nd_2O_3), and cobalt (II) acetate tetrahydrate ($Co(CH_3CO_2)_2{\cdot}4H_2O$), were analytical grade.

Particles surface modification by citrate treatment. A certain mass of each ferrite, suspended in sodium citrate solution 0.50 mol/L, was stirred with an ultrasonicator for 2 h at 60 °C to disperse any cluster of particles. By this treatment, the surface of the particles was modified to improve zinc hydroxide ($Zn(OH)_2$) coating. The two samples of modified ferrite particles were centrifuged and washed with acetone.

Zinc oxide precipitation. 10 mL of a zinc acetate dihydrate ($Zn(CH_3CO_2)_2{\cdot}2H_2O$) 0.55 mol/L solution and 10 mL of ammonium carbonate ($(NH_4)_2CO_3$) 0.80 mol/L were slowly and simultaneously added dropwise over 20 mL of surface-modified ferrites suspensions at 25 °C. This technique was adapted from a procedure previously published by Hong *et al.* to obtain a similar material [31].

Since magnetic stirring would cause aggregation of ferrite particles, the suspensions were mixed with nitrogen gas flow during the precipitation. The CO_2 released in the reaction also contributed to the stirring.

Due to the ammonium carbonate addition, the change in the pH caused the hydrated zinc oxide ($ZnO{\cdot}xH_2O$) to precipitate over the modified surface of the ferrite particles. The composites were centrifuged and washed with distilled water, diluted ammonia and absolute ethanol, and dried in a vacuum furnace. Then, they were heated for 4 h at 350 °C, to dehydrate the zinc oxide and gently milled.

These precipitations were done with different mass ratios between ferrite particles (either M00 or M20) and zinc acetate solution to prepare various samples. The names and nominal compositions of these samples are presented in **Table 1**. Finally, only two composites, labelled Z00 ($SrFe_{11}O_{19}/ZnO$) and Z20 ($Sr_{0.8}Nd_{0.2}Co_{0.2}Fe_{10.8}O_{19}/ZnO$), were chosen to carry out the kinetics experiments. All these samples were characterized by X-ray diffraction (XRD), scanning electron microscopy (SEM), and vibrating sample magnetometry (VSM).

Table 1. Nominal compositions of strontium ferrite/zinc oxide composites

Composite	Ferrite and its mass [mg/100 mg ZnO]	
M00	$SrFe_{11}O_{19}$	–
Z0L	M00	3
Z00	M00	45
Z01	M00	90
Z02	M00	178
Z20	M20	45

Kinetics measurements

Catalysts particles were suspended in distilled water. Orange II discoloration was scanned by visible light spectrophotometry. All experiments were performed at pH = 7.2.

Preparation of Orange II solution. Orange II (**Figure 1**) was prepared as its sodium salt by a coupling reaction between *beta*-naphtol (β-$C_{10}H_7OH$) and sulfanilic acid (*para*-aminebenzenesulfonic acid) in a sodium nitrite ($NaNO_2$) solution. Dye was recrystallized in ethanol-water, and 100 mg/L solution was made using distilled water.

Kinetics of photocatalyzed discoloration. Kinetics measurements were carried out with composites or ZnO suspensions. Control tests were performed on single ferrite particles or without light exposition. The results of the experiments are shown in **Table 2**. Samples for discoloration were prepared by mixing 4.00 mL of catalysts suspensions in distilled water (final conc. 1000 mg/L) and 1.00 mL dye solution (final conc. 20 mg/L).

Hydrated zinc oxide reacts either with hydronium or hydroxide ions [32]. Therefore, the pH is stabilized by combined acid-base/solubility equilibria of ZnO in the suspensions [33], which are presented here in equations (1)–(3) as follows:

$$ZnO \cdot x\,H_2O_{(s)} \rightleftharpoons Zn(OH)_{2\,(s)} + (x-1)\,H_2O_{(\ell)} \quad (1)$$

$$Zn(OH)_{2\,(s)} + 2\,H^+_{(aq)} \rightleftharpoons Zn^{2+}_{(aq)} + 2\,H_2O_{(\ell)} \quad (2)$$

$$Zn(OH)_{2\,(s)} + 2\,OH^-_{(aq)} \rightleftharpoons [Zn(OH)_4]^{2-}_{(aq)} \quad (3)$$

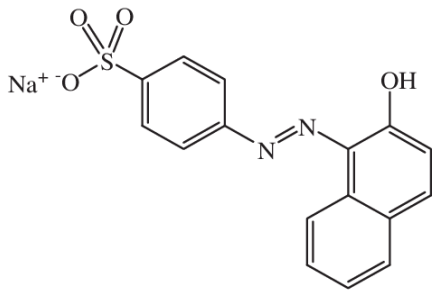

Figure 1. The azo dye Orange II as its sodium salt [34]

Table 2. Reactor tubes content in each discoloration experiment

Experiment #	Concentration [mg/L]		Light exposition
1	–	0	yes
2	–	0	no
3	M20	1000	yes
4	ZnO	1000	yes
5	ZnO	1000	no
6	Z00	100	yes
7	Z00	250	yes
8	Z00	1000	yes
9	Z20	1000	yes

Samples were placed into glass test tubes (1.5 cm diameter) of high optic quality and attached around the external surface of a borosilicate glass flask (15.0 cm diameter) in a carrousel-like array. A 160 W mixing lamp Philips ML was placed at the center of the flask, and the whole set was put into a thermostat water bath which could be mechanically stirred. The array of reactor tubes can be seen in **Figure 2**.

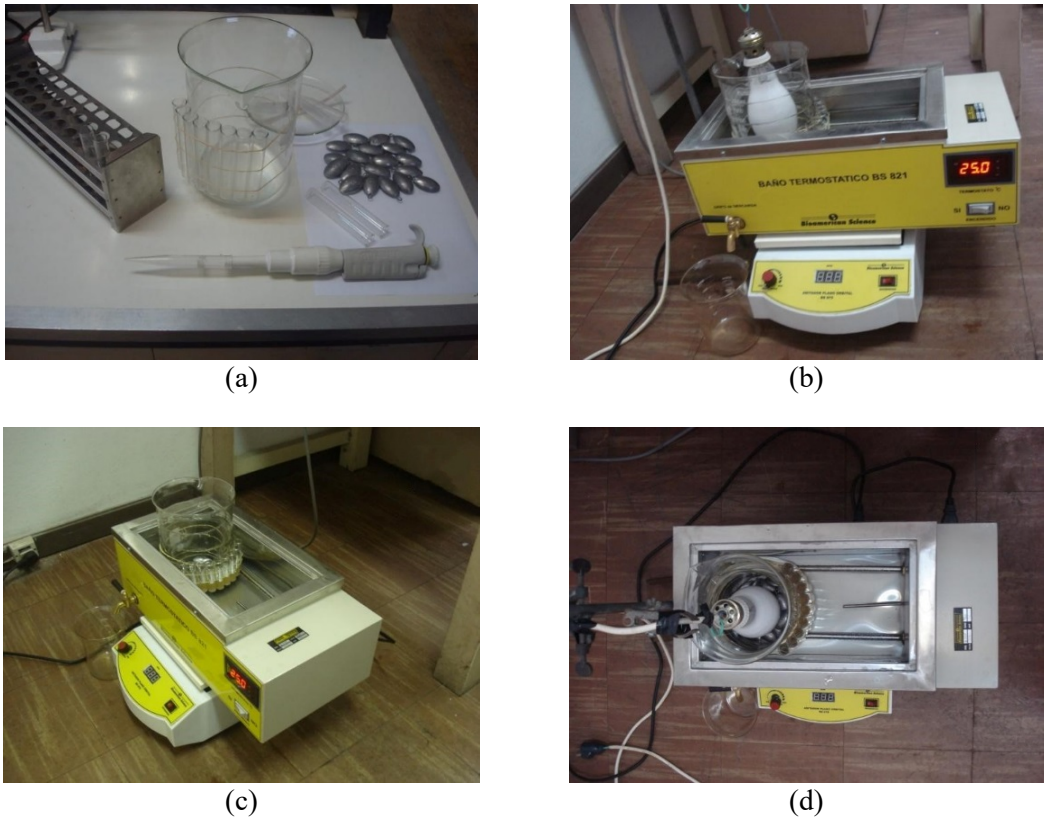

(a) (b)

(c) (d)

Figure 2. Images of the carrousel array of tubes around the flask and the mixing lamp (a–d)

Sunlight was emulated with this mixing lamp. Its emission combines a continuous spectrum of an incandescent tungsten filament and a line spectrum from a high-pressure

mercury source. During the kinetics experiments, the irradiance calculated value at the center of each test tube was 1900 W/m^2 approximately.

Light exposition and extraction of samples. All experiments were performed at 25 °C. Samples were homogenized in darkness by mechanical stirring and, immediately, all the test tubes were attached to the flask. At $t = 0$, the lamp was switched on; the first tube content was extracted with a syringe and centrifuged for 1 min at approx. 800 g (8000 m/s^2). The supernatant solution was put into a quartz cell; its absorbance was measured in a Shimadzu UV-2401 spectrophotometer at its maximum absorbance value within the visible spectrum, λ_{max} = 485 nm (reference: distilled water). This procedure was repeated with the next test tube after fixed intervals up to 240 min. Dye concentration values in each tube were calculated as a function of time using Lambert-Beer's law [35].

RESULTS AND DISCUSSION

Composites were structurally and magnetically characterized. Discoloration kinetics was studied by spectrophotometry.

Structural and magnetic characterization of the composites

XRD, SEM, and VSM were used to study the properties of the catalyst composites.

X-ray Diffractometry and Scanning Electron Microscopy results. The XRD patterns of all the composites, measured in a Philips diffractometer (using Cu$K\alpha$ radiation), are shown in Figure 3. The profiles confirm the hexagonal phase of Sr ferrite and the main peaks assigned to ZnO.

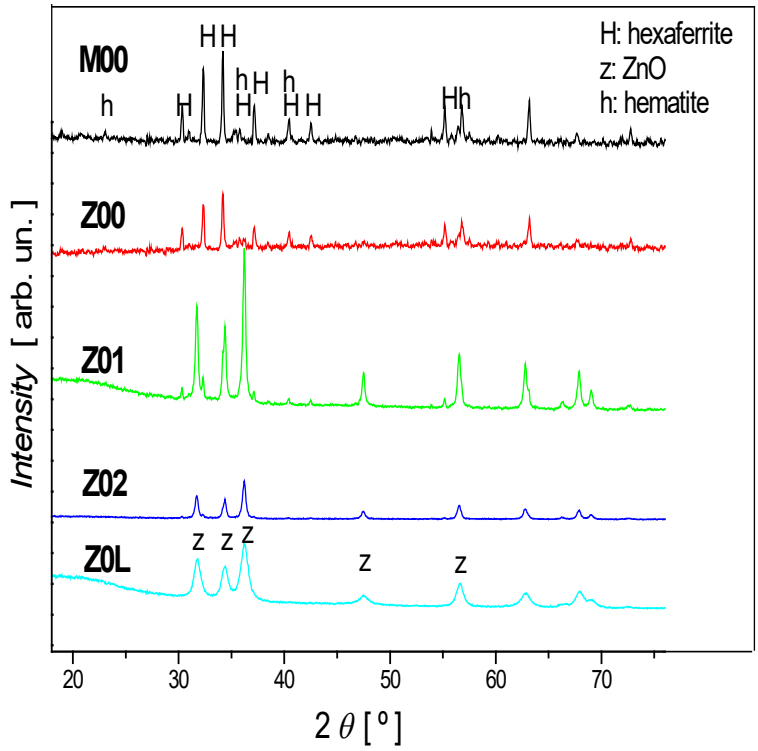

Figure 3. X-ray diffractograms of M00 (Sr hexaferrite) and all the composites

Strontium hexaferrite, Z00 composite ($SrFe_{11}O_{19}$/ZnO), and zinc oxide nanoparticles were structurally characterized by SEM in a Zeiss DSM 982 GEMINI microscope. **Figure 4** shows the SEM images. The hexagonal ferrite looks like platelets (average particle size 230 nm), while the ZnO nanoparticles are spherical and well dispersed (average particle size 60 nm).

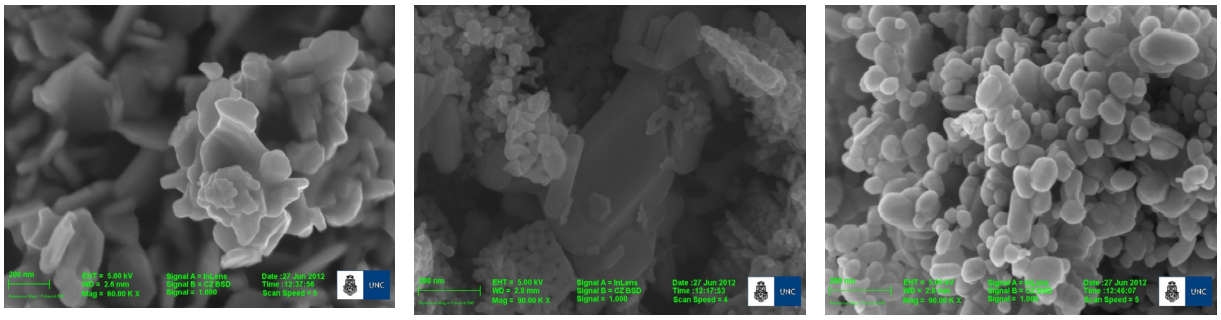

(a) (b) (c)

Figure 4. SEM images, magnified × 90000: M00 Sr hexaferrite (a); Z00 composite (b); and ZnO nanoparticles (c)

Magnetic measurements. Magnetization *versus* magnetic field (*M-H*) loops of the M00/ZnO composites were measured with a Lakeshore 7300 VSM, and their main magnetic properties were calculated (**Table 3**). Magnetic results of M20/ZnO composite (Z20) are not presented.

Table 3. Magnetic properties values of the composites

Sample	Saturation magnetization, M_S [Am^2/kg]	Coercive field, H_C [A/m]
M00 ferrite	97	62.0
Z0L	0.7	65.8
Z00	7.2	53.5
Z01	15.1	52.6
Z02	76	43.2

Since magnetization of a two-component system depends on component masses **[36]** and zinc oxide is a diamagnetic material, it is possible to ponderate mass composition from M_S results. In this way, for the Z00 composite, a ZnO mass fraction of 0.926 was calculated. The enhancement in H_C for the Z0L composite is related to the high dilution of the ferrite particles into a non-magnetic material. These composites show good magnetic properties after the one-step preparation method.

Kinetics of Orange II dye photocatalyzed discoloration

Preliminary experiments to explore/discard Orange II adsorption on catalyst were performed. The absorbance of azo dye solutions with and without ZnO nanopowder was measured in darkness. Besides, Orange II stability was tested with M20 ferrite (without ZnO coating) suspended particles. Results are presented in **Figure 5**. All these profiles show a very small negative slope, so it can be concluded that dye adsorption on ZnO particles or the magnetic support is negligible (< 0.3%). These experiments show that neither ZnO nanoparticles nor Sr ferrite particles diminish Orange II concentration by adsorption processes.

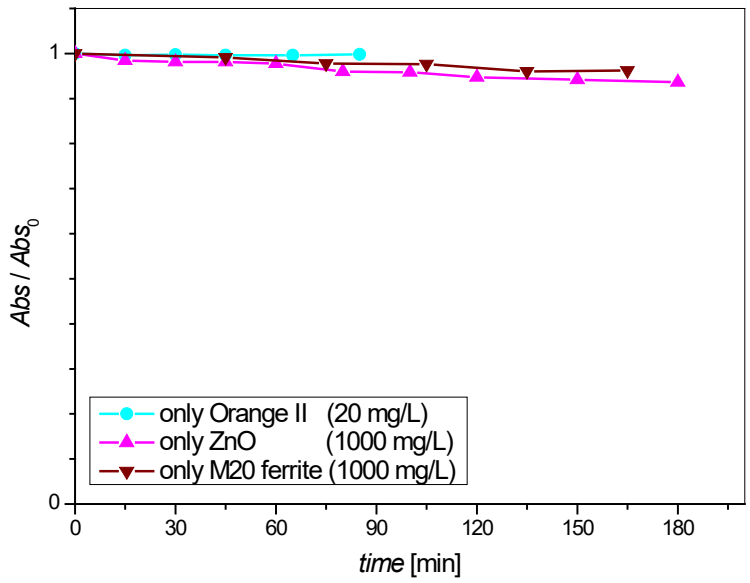

Figure 5. Orange II adsorption on ZnO or M20 nanoparticles

Strontium ferrite/zinc oxide composites kinetics experiments. **Figure 6** shows dye absorbance at 485 nm in the centrifuged Z00 composite supernatants divided by the initial value, $Abs(t)/Abs_0$ vs. time. By Lambert-Beer's law, these relative absorbances should be equal to the relation $C(t)/C_0$, between the concentration at any time and the initial concentration at the beginning of the light exposition. Orange II solution behaviour without any catalyst is included for comparison (Experiment #1 – **Table 2**).

It can be seen in **Figure 6** that dye concentration slightly varies in the absence of catalyst (orange symbol), whereas suspended Z00 catalyst particles (blue symbols) cause an exponential decay in the azo dye absorbance. This type of curve would match with a first-order kinetics reaction.

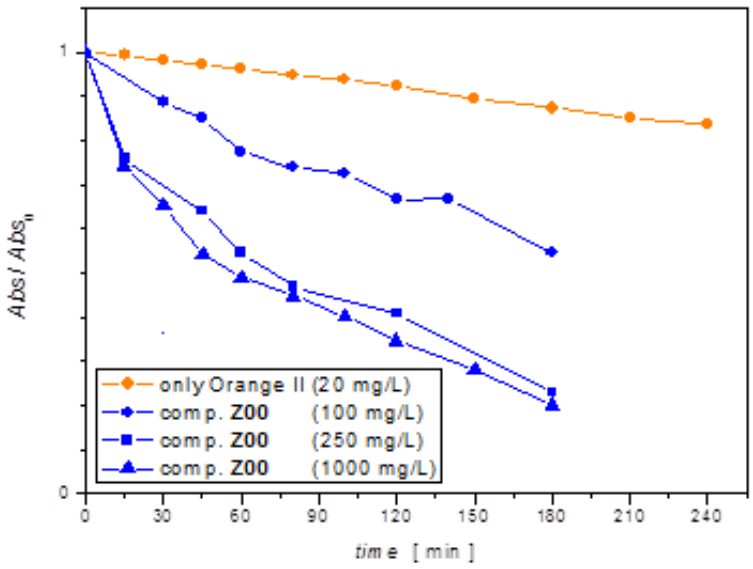

Figure 6. Orange II / Z00 composite discoloration with light exposition

Figure 7 shows $Abs(t)/Abs_0$ values as a function of time for the kinetics experiments carried out with 1000 mg/L of Z00, Z20, or ZnO nanoparticles suspended in the Orange II 20 mg/L solution.

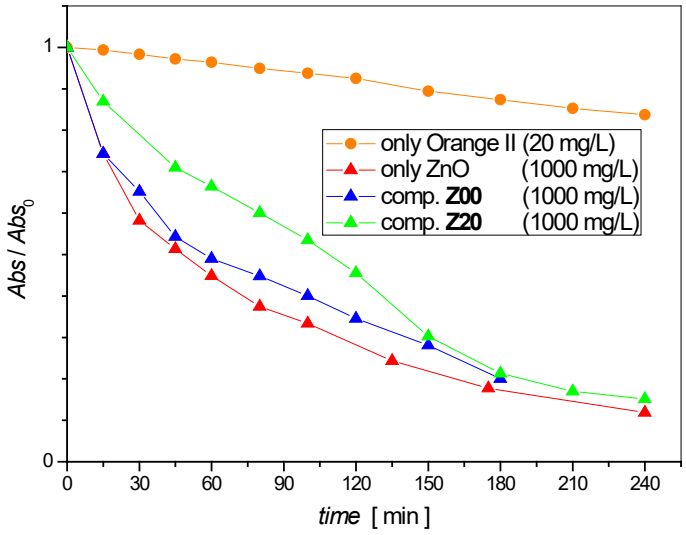

Figure 7. Orange II / Z00 or Z20 composites and zinc oxide discoloration with light exposition (for comparison Orange II is included)

It can be seen in **Figure 7** that Z00 composite and single zinc oxide suspended particles cause similar absorbance exponential decays. The Z20 composite (Nd-Co substituted strontium ferrite) curve presents a similar profile, although its initial slope is less negative than the others.

Kinetics of all photocatalytic reactions agreed with a first-order law, as Marto and other authors had found using only ZnO **[8]**. The first-order reaction rate constant (k_1) and half-life ($t_{½}$) parameters were calculated from the initial slopes of relative absorbance logarithmic graphs. These values are shown in **Table 4**.

Table 4. Kinetics parameters calculated from the experiments (T = 25 °C)

Experiment #	Description	Slope, k_1 [1/min]	$t_{½} = ln\ 2 / k_1$ [min]
4	ZnO 1000 mg/L	0.0161	43.0
6	Z00 100 mg/L	0.0037	187
7	Z00 250 mg/L	0.0107	64.7
8	Z00 1000 mg/L	0.0142	48.8
9	Z20 1000 mg/L	0.0078	89.1

The $t_{½}$ values for the 1000 mg/L catalyst suspensions were 49 min for Z00 composite and 90 min for Z20 composite. Then, the rate of the reaction catalyzed by composites decreased compared with that of the ZnO suspension with the same nominal concentration ($t_{½}$ = 43 min).

However, it should be considered that suspensions of Z00 composite have a real mass of zinc oxide 7.4% less than their nominal composition (ZnO mass fraction = 0.926). Therefore, it should be concluded that the decrease in the reaction rate using the composite instead of single ZnO should be lesser than the previously calculated value.

It can be seen in **Figure 6** that the initial rate is related to the catalyst concentration up to a value of 250 mg/L. For a higher catalyst concentration (1000 mg/L), the discoloration rates behave similarly for both hexaferrite composites after 180 min, although their initial rates are

somewhat different (**Figure 7**). It is noticeable that the Sr ferrite supported catalyst (blue symbol) presents a similar behaviour as single ZnO nanoparticles (red symbol).

No other analytical technique was used in this work to measure any degradation products from the Orange II. However, as control experiments in darkness showed no significant azo dye adsorption, we proposed that the main discoloration process should be the catalyzed oxidation of the azo group with light exposition. It can also be inferred that photocatalyzed azo dye reaction should be the same with all the tested catalysts, magnetic composites, or suspended ZnO nanopowders.

Effect of catalyst concentration on Orange II discoloration. **Figure 8** shows reaction rate constant k_1 values obtained from the experiments with ZnO powder and Z00 composite vs. catalyst loading. Within the tested range of catalyst concentration, the value of k_1 for the ZnO powder measurements increases linearly with the catalyst load. However, the rate-constant increment in Z00 experiments becomes less steep for amounts of suspended composite greater than 250 mg/L. This behaviour has already been reported and analyzed by Sakthivel *et al.* **[37]**.

At first, a linear rise in the rate constant with the amount of catalyst is observed. This has been attributed to the increase of active sites on the photocatalyst surface, which results in a greater generation of •OH radicals, that would oxidize more azo dye molecules. But, as Nishio *et al.* found, for ZnO concentrations between 1000 and 1500 mg/L, the slope substantially decreases, and the rate constant becomes nearly independent of the catalyst load **[3]**.

It has been reported by Kaur *et al.* that the increment of solution turbidity would hinder light transmission due to the significant scattering, and there would be no longer increment of hydroxide radical generation **[38]**. Therefore, there is an optimal level of zinc oxide concentration, and a further increase of the catalyst load will not be effective. This optimal value would seem smaller for the Z00 composite (between 250 and 1000 mg/L), probably due to a more intensive scattering of the suspended ferrite particles.

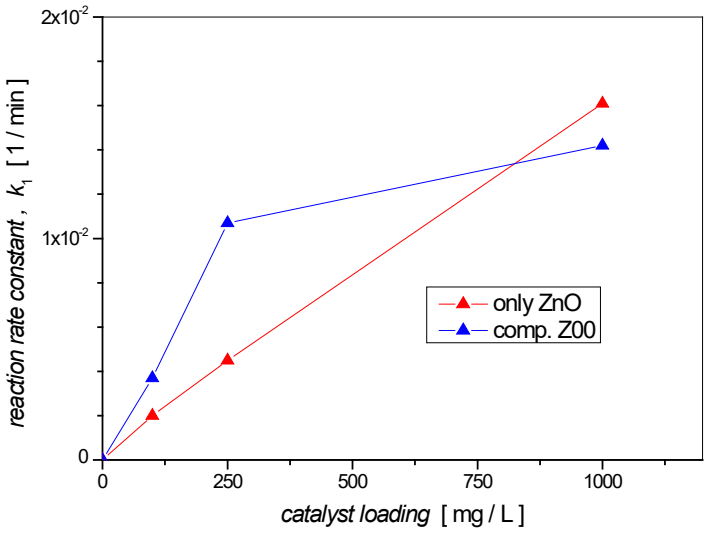

Figure 8. Variation of rate constant with catalyst loading

Remotion of the photocatalyst from water suspension

The suspended photocatalysts were removed from dye solutions by magnetic decantation with an iron-neodymium-boron (Fe-Nd-B) alloy magnet and then dried and weighed **[39]**. Composites were recovered with an average factor of 70%. This magnetic removal was carried out as a lab procedure and has not been tested at an industrial scale. Probably, there would be no severe disadvantages of the usage and recovery of a photocatalyst supported on magnetic

particles in an industrial application since similar techniques have already been published and patented [40]. These procedures included the remotion of magnetic particles from seawater [41].

CONCLUSIONS

Composites prepared with ZnO precipitated nanoparticles on hexaferrite magnetic particles (Sr ferrite and Nd–Co substituted Sr ferrite) were successfully synthesized by a one-step coprecipitation method. These composites retain their magnetic properties after preparation at neutral pH. SEM images show that zinc oxide nanoparticles cannot completely coat Sr ferrite particles, although they seem to be steadily attached to the hard magnetic phase.

ZnO nanopowders and the prepared composites were tested as photocatalysts for Orange II dye discoloration in aqueous solution at 25 °C with light exposition at pH = 7.2. Preliminary experiments performed in darkness showed that the adsorption of the azo dye over ZnO or ferrite particles is negligible.

The synthesized composites present good catalyst properties in the photocatalyzed discoloration of the pollutant Orange II compared to single zinc oxide nanoparticles dispersed in water at the same experimental conditions. First-order reaction rate coefficients and half-life values calculated for Sr ferrite/ZnO composites are quite similar to those observed with zinc oxide nanopowder. The Nd-Co substituted Sr ferrite/ZnO catalyst showed the lowest catalytic activity, but its kinetics parameters were good enough to achieve a significant azo dye discoloration.

Composite particles can be easily removed from the water, by magnetic decantation, with a significant recovery factor (70%). These preliminary results indicate that these supported magnetic catalysts can be satisfactorily employed for industrial remediation. The influence of ZnO particle size on the photocatalytic activity of these composites and the re-use of the recovered catalyst particles will be studied in further experiments.

ACKNOWLEDGMENTS

The authors are indebted to Dra. Paula Bercoff for the structural and magnetic characterization of the composites, and to Dra. Nora François for the use of the spectrophotometer. The University of Buenos Aires (grant UBACyT 01–Q603BA) supported this work.

NOMENCLATURE

Abs	absorbance	[-]
C	concentration	[mg/L]
g	gravitational acceleration	[m/s^2]
H_C	coercive field	[A/m]
k_1	reaction rate constant	[1/min]
M_S	saturation magnetization	[Am^2/kg]
T	temperature	[°C]
t	time	[min]
$t_{½}$	half-life	[min]

Greek letters

λ	wavelength	[nm]
θ	diffraction angle	[°]

Subscripts

max	maximum
0	initial

Abbreviations

SEM	Scanning Electron Microscopy
VSM	Vibrating Sample Magnetometry
XRD	X-Ray Diffractometry

REFERENCES

1. N. Daneshvar, M. H. Rasoulifard, A. R. Khataee, and F. Hosseinzadeh, "Removal of C.I. Acid Orange 7 from aqueous solution by UV irradiation in the presence of ZnO nanopowder," J. Hazard. Mater., vol. 143, no. 1–2, pp. 95–101, 2007, https://doi.org/10.1016/j.jhazmat.2006.08.072
2. W. Z. Khan, I. Najeeb, and S. Ishtiaque, "Photocatalytic Degradation of a Real Textile Wastewater Using Titanium Dioxide, Zinc Oxide and Hydrogen Peroxide," Int. J. Eng. Sci., vol. 5, no. 7, pp. 61–70, 2016
3. J. Nishio, M. Tokumura, H. T. Znad, and Y. Kawase, "Photocatalytic Decolorization of Azo-dye with Zinc Oxide Powder in an External UV Light Irradiation Slurry Photoreactor," J. Hazard. Mater., vol. 138, no. 1, pp. 106–115, 2006, https://doi.org/10.1016/j.jhazmat.2006.05.039
4. N. Daneshvar, D. Salari, and A. R. Khataee, "Photocatalytic Degradation of Azo Dye Acid Red 14 in Water on ZnO as an Alternative Catalyst to TiO2," J. Photochem. Photobiol. A Chem., vol. 162, no. 2–3, pp. 317–322, 2004, https://doi.org/10.1016/S1010-6030(03)00378-2
5. P. Gonçalves, R. Bertholdo, J. A. Dias, S. C. Maestrelli, and T. R. Giraldi, "Evaluation of the Photocatalytic Potential of TiO2 and ZnO Obtained by Different Wet Chemical Methods," Mater. Res. - Iberoam. J. Mater., vol. 20, no. 2, pp. 181–189, 2017, https://doi.org/10.1590/1980-5373-MR-2016-0936
6. C. B. Ong, L. Y. Ng, and A. W. Mohammad, "A Review of ZnO Nanoparticles as Solar Photocatalysts: Synthesis, Mechanisms and Applications," Renew. Sustain. Energy Rev., vol. 81, pp. 536–551, 2018, https://doi.org/10.1016/j.rser.2017.08.020
7. C. S. Lin, C. C. Hwang, W. H. Lee, and W. Y. Tong, "Preparation of Zinc Oxide (ZnO) Powders with Different Types of Morphology by a Combustion Synthesis Method," Mater. Sci. Eng. B, vol. 140, no. 1–2, pp. 31–37, 2007, https://doi.org/10.1016/j.mseb.2007.03.023
8. J. Marto, P. São Marcos, T. Trindade, and J. A. Labrincha, "Photocatalytic Decolouration of Orange II by ZnO Active Layers Screen-printed on Ceramic Tiles," J. Hazard. Mater., vol. 163, no. 1, pp. 36–42, 2009, https://doi.org/10.1016/j.jhazmat.2008.06.056
9. A. M. Ali, E. A. C. Emanuelsson, and D. A. Patterson, "Photocatalysis with Nanostructured Zinc Oxide Thin Films: The Relationship between Morphology and Photocatalytic Activity under Oxygen Limited and Oxygen Rich Conditions and Evidence for a Mars Van Krevelen Mechanism," Appl. Catal. B Environ., vol. 97, no. 1–2, pp. 168–181, 2010, https://doi.org/10.1016/j.apcatb.2010.03.037
10. S. Danwittayakul, M. Jaisai, T. Koottatep, and J. Dutta, "Enhancement of Photocatalytic Degradation of Methyl Orange by Supported Zinc Oxide Nanorods/Zinc Stannate (ZnO/ZTO) on Porous Substrates," Ind. Eng. Chem. Res., vol. 52, no. 38, pp. 13629–13636, 2013, https://doi.org/10.1021/ie4019726
11. A. Sáenz-Trevizo et al., "On the Discoloration of Methylene Blue by Visible Light," J. Fluoresc., vol. 29, no. 1, pp. 15–25, 2019, https://doi.org/10.1007/s10895-018-2304-6
12. S. Wang, P. Kuang, B. Cheng, J. Yu, and C. Jiang, "ZnO Hierarchical Microsphere for Enhanced Photocatalytic Activity," J. Alloys Compd., vol. 741, pp. 622–632, 2018, https://doi.org/10.1016/j.jallcom.2018.01.141
13. J. Liu, Y. Zhao, J. Ma, Y. Dai, J. Li, and J. Zhang, "Flower-like ZnO Hollow Microspheres on Ceramic Mesh Substrate for Photocatalytic Reduction of Cr(VI) in Tannery

Wastewater," Ceram. Int., vol. 42, no. 14, pp. 15968–15974, 2016, https://doi.org/10.1016/j.ceramint.2016.07.098
14. A. Balcha, O. P. Yadav, and T. Dey, "Photocatalytic Degradation of Methylene Blue Dye by Zinc Oxide Nanoparticles Obtained from Precipitation and Sol-gel Methods," Environ. Sci. Pollut. Res., vol. 23, no. 24, pp. 25485–25493, 2016, https://doi.org/10.1007/s11356-016-7750-6
15. N. Sharma, R. Jha, S. Baghel, and D. Sharma, "Study on Photocatalyst Zinc Oxide Annealed at Different Temperatures for Photodegradation of Eosin Y dye," J. Alloys Compd., vol. 695, pp. 270–279, 2017, https://doi.org/10.1016/j.jallcom.2016.10.194
16. S. S. Kumar, P. Venkateswarlu, V. R. Rao, and G. N. Rao, "Synthesis, Characterization and Optical Properties of Zinc Oxide Nanoparticles," Int. Nano Lett., vol. 3, no. 30, pp. 1–6, 2013, https://doi.org/10.1186/2228-5326-3-30
17. J. Govan and Y. Gun'ko, "Recent Advances in the Application of Magnetic Nanoparticles as a Support for Homogeneous Catalysts," Nanomaterials, vol. 4, no. 2, pp. 222–241, 2014, https://doi.org/10.3390/nano4020222
18. A. R. Faraji, S. Mosazadeh, and F. Ashouri, "Synthesis and Characterization of Cobalt-supported Catalysts on Modified Magnetic Nanoparticle: Green and Highly Efficient Heterogeneous Nanocatalyst for Selective Oxidation of Ethylbenzene, Cyclohexene and Oximes with Molecular Oxygen," J. Colloid Interface Sci., vol. 506, pp. 10–26, 2017, https://doi.org/10.1016/j.jcis.2017.06.100
19. F. Wu, B. J. Harper, and S. L. Harper, "Comparative Dissolution, Uptake, and Toxicity of Zinc Oxide Particles in Individual Aquatic Species and Mixed Populations," Environ. Toxicol. Chem., vol. 38, no. 3, pp. 591–602, 2019, https://doi.org/10.1002/etc.4349
20. R. Bacchetta, B. Maran, M. Marelli, N. Santo, and P. Tremolada, "Role of Soluble Zinc in ZnO Nanoparticle Cytotoxicity in Daphnia magna: A Morphological Approach," Environ. Res., vol. 148, pp. 376–385, 2016, https://doi.org/10.1016/j.envres.2016.04.028
21. M. Chevallet et al., "Metal Homeostasis Disruption and Mitochondrial Dysfunction in Hepatocytes Exposed to Sub-toxic Doses of Zinc Oxide Nanoparticles," Nanoscale, vol. 8, no. 43, pp. 18495–18506, 2016, https://doi.org/10.1039/c6nr05306h
22. V. Kononenko et al., "Comparative in vitro Genotoxicity Study of ZnO Nanoparticles, ZnO Macroparticles and ZnCl2 to MDCK Kidney Cells: Size Matters," Toxicol. Vitr., vol. 40, pp. 256–263, 2017, https://doi.org/10.1016/j.tiv.2017.01.015
23. K. K. Kefeni, B. B. Mamba, and T. A. M. Msagati, "Application of Spinel Ferrite Nanoparticles in Water and Wastewater Treatment: A Review," Sep. Purif. Technol., vol. 188, pp. 399–422, 2017, https://doi.org/10.1016/j.seppur.2017.07.015
24. C. Cai, J. Liu, Z. Zhang, Y. Zheng, and H. Zhang, "Visible Light Enhanced Heterogeneous Photo-degradation of Orange II by Zinc Ferrite (ZnFe2O4) Catalyst with the Assistance of Persulfate," Sep. Purif. Technol., vol. 165, pp. 42–52, 2016, https://doi.org/10.1016/j.seppur.2016.03.026
25. K. Zhu, J. Wang, Y. Wang, C. Jin, and A. S. Ganeshraja, "Visible-light-induced Photocatalysis and Peroxymonosulfate Activation over ZnFe2O4 Fine Nanoparticles for Degradation of Orange II," Catal. Sci. Technol., vol. 6, no. 7, 2016, https://doi.org/10.1039/c5cy01735a
26. A. Tadjarodi, M. Imani, and M. Salehi, "ZnFe2O4 Nanoparticles and a Clay Encapsulated ZnFe2O4 Nanocomposite: Synthesis Strategy, Structural Characteristics and the Adsorption of Dye Pollutants in Water," RSC Adv., vol. 5, no. 69, pp. 56145–56156, 2015, https://doi.org/10.1039/c5ra02163d
27. A. L. S. Coelho, A. F. de Almeida Neto, F. F. Ivashita, G. G. Lenzi, L. M. M. de Jorge, and O. A. A. dos Santos, "Characterization-performance of ZnO and ZnO/ZnFe2O4 Catalyst Using Artificial and Solar Light for Mercury (II) Reduction," Brazilian J. Chem. Eng., vol. 36, no. 2, pp. 797–810, 2019, https://doi.org/10.1590/0104-6632.20190362s20180280

28. S. Mandal and S. Natarajan, "Adsorption and Catalytic Degradation of Organic Dyes in Water Using ZnO/ZnxFe3-xO4 Mixed Oxides," J. Environ. Chem. Eng., vol. 3, no. 2, pp. 1185–1193, 2015, https://doi.org/10.1016/j.jece.2015.04.021
29. M. L. Maya-Treviño, M. Villanueva-Rodríguez, J. L. Guzmán-Mar, L. Hinojosa-Reyes, and A. Hernández-Ramírez, "Comparison of the Solar Photocatalytic Activity of ZnO–Fe2O3 and ZnO–Fe(0) on 2,4-D Degradation in a CPC Reactor," Photochem. Photobiol. Sci., vol. 14, no. 3, pp. 543–549, 2015, https://doi.org/10.1039/c4pp00274a
30. C. A. Herme, P. G. Bercoff, and S. E. Jacobo, "Nd–Co Substituted Strontium Hexaferrite Powders with Enhanced Coercivity," Mater. Res. Bull., vol. 47, no. 11, pp. 3881–3887, 2012, https://doi.org/10.1016/j.materresbull.2012.08.047
31. R. Y. Hong et al., "Preparation, Characterization and Application of Fe3O4/ZnO Core/Shell Magnetic Nanoparticles," Mater. Res. Bull., vol. 43, no. 8–9, pp. 2457–2468, 2008, https://doi.org/10.1016/j.materresbull.2007.07.035
32. J. N. Butler and D. R. Cogley, Ionic Equilibrium: Solubility and pH Calculations, Revised Ed. Hoboken, New Jersey: Wiley-Interscience, 1998
33. M. Aguilar Sanjuán, Introduction to Ionic Equilibria (in Spanish), 2nd ed. Barcelona, Spain: Reverté Ed., 1999
34. F.-C. Tsai et al., "Adsorptive Removal of Acid Orange 7 from Aqueous Solution with Metal–organic Framework Material, Iron (III) Trimesate," Desalin. Water Treat., vol. 57, no. 7, pp. 3218–3226, Nov. 2016, https://doi.org/10.1080/19443994.2014.982199
35. D. A. Skoog, D. M. West, F. J. Holler, and S. R. Crouch, Analytical Chemistry: An Introduction, 7th ed. Orlando, Florida: Harcourt Inc., 2000
36. B. D. Cullity and C. D. Graham, Introduction to Magnetic Materials, 2nd ed. Hoboken, New Jersey: John Wiley & Sons Inc.–IEEE Press, 2009
37. S. Sakthivel, B. Neppolian, M. V. Shankar, B. Arabindoo, M. Palanichamy, and V. Murugesan, "Solar Photocatalytic Degradation of Azo Dye: Comparison of Photocatalytic Efficiency of ZnO and TiO2," Sol. Energy Mater. Sol. Cells, vol. 77, no. 1, pp. 65–82, 2003, https://doi.org/10.1016/S0927-0248(02)00255-6
38. J. Kaur, S. Bansal, and S. Singhal, "Photocatalytic Degradation of Methyl Orange Using ZnO Nanopowders Synthesized via Thermal Decomposition of Oxalate Precursor Method," Phys. B Condens. Matter, vol. 416, pp. 33–38, 2013, https://doi.org/10.1016/j.physb.2013.02.005
39. C. A. Herme, "Preparation, Characterization and Properties of New Nd–Co Magnetic Materials (in Spanish)," University of Buenos Aires (UBA), Buenos Aires, Argentina, 2017
40. R. Kaiser, "Process for Cleaning Up Oil Spills," US 3635819 A, 1972
41. M. Zahn, T. A. Hatton, and S. R. Krushrushahi, "Magnetic Colloid Petroleum Oil Spill Clean-up of Ocean Surface, Depth, and Shore Regions," WO 2012/115814 A1, 2012

Paper submitted: 08.10.2020
Paper revised: 02.04.2021
Paper accepted: 08.04.2021